



Contents lists available at ScienceDirect

Journal of Controlled Release

journal homepage: www.elsevier.com/locate/jconrel

Sunlight triggered photodynamic ultradeformable liposomes against *Leishmania braziliensis* are also leishmanicidal in the dark

Jorge Montanari^a, Cristina Maidana^b, Mónica Inés Esteva^b, Cristina Salomon^c, Maria Jose Morilla^a, Eder L. Romero^{a,*}

^a Programa de Nanomedicinas, Departamento de Ciencia y Tecnología, Universidad Nacional de Quilmes, Roque Saenz Peña 352, Bernal, B1876 BXD, Buenos Aires, Argentina

^b Instituto Nacional de Parasitología Dr. Mario Fatala Chaben, Paseo Colon 568, 1063, Buenos Aires, Argentina

^c Área Microbiología, Facultad de Ciencias Médicas, Universidad Nacional de Cuyo. Av. Libertador 80. Centro Universitario, 5500, Mendoza. Argentina

ARTICLE INFO

Article history:

Received 15 June 2010

Accepted 11 August 2010

Available online xxxx

Keywords:

Ultradeformable liposomes

Cutaneous leishmaniasis

Photodynamic therapy

Transcutaneous

ABSTRACT

Being independent of artificial power sources, self administered sunlight triggered photodynamic therapy 22 could be suitable alternative treatment for cutaneous leishmaniasis, that avoids the need for injectables 23 and the toxic side effects of pentavalent antimonials. In this work we have determined the *in vitro* 24 leishmanicidal activity of sunlight triggered photodynamic ultradeformable liposomes (UDL). ZnPc is a 25 hydrophobic Zn phthalocyanine that showed 20% anti-promastigote activity (APA) and 20% anti- 26 amastigote activity (AA) against *Leishmania braziliensis* (strain 2903) after 15 min sunlight irradiation 27 (15 J/cm²). However, when loaded in UDL as UDL-ZnPc (1.25 μM ZnPc–1 mM phospholipids) it elicited 28 100% APA and 80% AA at the same light dose. In the absence of host cell toxicity, UDL and UDL-ZnPc also 29 showed non-photodynamic leishmanicidal activity. Confocal laser scanning microscopy of cryosectioned 30 human skin mounted in non-occlusive Saarbrücken Penetration Model, showed that upon transcutaneous 31 administration ZnPc penetrated nearly 10 folds deeper as UDL-ZnPc that if loaded in conventional 32 liposomes. Quantitative determination of ZnPc confirmed that UDL-ZnPc penetrated homogeneously in 33 the *stratum corneum*, carrying 7 folds higher amount of ZnPc 8 folds deeper than L-ZnPc. It is envisioned 34 that the multiple leishmanicidal effects of UDL-ZnPc could play a synergistic role in prophylaxis or 35 therapeutic at the first stages of the infection. 36

© 2010 Published by Elsevier B.V. 37

1. Introduction

Cutaneous (CL) and mucocutaneous leishmaniasis (MCL) are 43 clinical manifestations of a group of diseases caused by dimorphic 44 protozoa that belong to different species of the *Leishmania* genus, [1] 45 which are transmitted to humans by sandfly bites. Infective parasites 46 are hosted in skin macrophages and produce ulcerative lesions [2] as 47 well as destructive mucosa inflammation in MCL [3]. 1.5 million new 48 cases of CL arise worldwide each year [4], presenting a complex 49 epidemiology that depends on intra and inter species variations [5]. The 50 CL's geographic incidence is heterogeneous, including densely affected 51 foci and dissemination areas in constant change [6] due to emigrations, 52 tourism [7,8], urbanization [9] and the expansion of suitable ecosys- 53 tems for the vector due to climatic changes [10]. A marked increase of 54 cases in Europe and America has been recorded in the last decades, and 55 new important epidemic foci have emerged [4,11].

Standard treatment are based on systemic or intralesional 56 administration of pentavalent antimonials according to the species 57

and the clinical symptoms (intravenous or intramuscular 20–50 mg 59 Sb(v)/kg weight/day for 30 days, or 1–3 ml under the edge of lesion 60 and entire lesion every 5–7 days for a total of 2–5 times [12], systemic 61 amphotericin B and pentamidine isothionate [13,14]. The response to 62 the treatment is slow and even inefficacious according to the species, 63 with incomplete cure and relapse occurring within 6 months [13]. 64 Treatments are linked to side effects such as hepatic alterations, 65 biochemical pancreatitis, flattening of T waves in ECG, myalgia, 66 arthralgia, thrombocytopenia, transient suppression of bone marrow 67 and reversible renal insufficiency [15]. 68

Thus, a search for an effective, simple, and low-cost treatment for 69 CL that can be administered conveniently is still an active topic. In this 70 scenario, topical treatment is preferable to systemic interventions 71 [16]. The highly hydrophilic antibiotic paromomycin ointment (15%) 72 associated to the permeation enhancer methyl benzethonium 73 chloride (12%) (MBC), are relatively effective for CL treatment (*L* 74 *major*, *L. tropica*, *L. mexicana* and *L. panamensis*), but local side effects 75 are observed frequently due to MBC [17]. On the other hand, topical 76 amphotericin B (Amphocil in 5% ethanol) has been successful in 77 treatment of *L. major* infected patients in Israel [18,19], but the high 78 cost of Amphocil restricts the use to patients and more extensive 79 studies are needed. 80

* Corresponding author. Tel.: +54 1143657100; fax: +54 1143657132.
E-mail address: elromero@unq.edu.ar (E.L. Romero).

Photodynamic therapy (PDT) is a potentially applicable, safe and affordable technology that is currently in use for the treatment of cancer and aged-related macular degeneration. PDT is based on the concept that a photoactivatable compound, called a photosensitizer, can be excited by light of the appropriate wavelength to generate cytotoxic singlet oxygen and free radicals [20]. PDT is an attractive option to conventional antimicrobial chemotherapy, since it does not induce resistant strains neither upon multiple treatments [21,22]. Although PDT has rendered several cases of CL clinical cure with good cosmetic results [23,24], the lack of standardized data and the needs for special medical equipment (lamps), have hampered the use of PDT against CL [25]. The use of daylight to PDT can be an alternative to this last drawback. Recently a Phase II clinical trial in Israel has been started to determine the efficiency of methyl aminolevulinate (MAL)-PDT daylight triggered for the treatment of CL (*L. major* and *L. tropica*) [26].

In the present work, we have determined the *in vitro* leishmanicidal activity of the hydrophobic photosensitizer Zn phthalocyanine (ZnPc) loaded in ultradeformable liposomes (UDL-ZnPc) both in the darkness and upon sunlight irradiation and screened the ability of UDL-ZnPc to penetrate intact skin.

2. Materials and methods

2.1. Materials

Soybean phosphatidylcholine (SPC) (phospholipon 90 G, purity >90%) was a gift from Phospholipid/Natterman, Germany. Sodium cholate (NaChol), 1,2-Dimyristoyl-*sn*-glycero-3-phosphoethanolamine-N-(Lissamine™ rhodamine B sulfonyl) (Rh-PE), and Sephadex G-50 were purchased from Sigma-Aldrich, Argentina. The fluorophore 8-hydroxypyrene-1,3,6-trisulfonic acid (HPTS) was from Molecular Probes (Eugene, OR, USA). Q-tracker non-targeted Quantum Dots 655, with a *core/shell* of CdSe/ZnS covered by PEG (QD) was from Invitrogen (Hayward, CA). The hydrophobic ([tetrakis(2,4-dimethyl-3-pentyloxi)-phthalocyaninate]zinc(II)) Zn phthalocyanine (ZnPc) was synthesized as described in Montanari et al. [27]. Other reagents were analytic grade from Anedra, Argentina.

2.2. Preparation and characterization of ultradeformable liposomes

UDL and UDL-ZnPc were prepared as stated in Montanari et al. [27]. Briefly, UDL composed of SPC and NaChol at 6:1 (w/w) ratio, were prepared by mixing lipids from CHCl₃ and CHCl₃:CH₃OH (1:1, v/v) solutions, respectively, that were further rotary evaporated at 40 °C in round bottom flask until organic solvent elimination. The thin lipid film was flushed with N₂, and hydrated in 10 mM Tris-HCl buffer plus 0.9% (w/v) NaCl, pH 7.4 (Tris buffer), up to a final concentration of 43 mg SPC/ml. The suspension was sonicated (45 min with a bath type sonicator 80 W, 40 kHz) and extruded 15 times through two stacked 0.2 and 0.1 μm pore size polycarbonate filters using a 100 ml Thermobarrel extruder (Northern Lipids, Canada). ZnPc was co-solubilized in the organic solution with lipids (2 mg ZnPc/g SPC) to prepare UDL-ZnPc.

Conventional – non ultradeformable, without NaChol – liposomes (L) were prepared by the same procedure.

Liposomal phospholipids were quantified by a colorimetric phosphate micro assay [28]. Mean particle size of each liposomal preparation was determined by dynamic light scattering with Nanozetasizer (Malvern).

2.3. Cytotoxicity on mammal cells

2.3.1. Lactate dehydrogenase (LDH) assay

J-774 and Vero cells were maintained at 37 °C with 5% CO₂, in RPMI 1640 medium supplemented with 10% heat-inactivated FCS, 2 mM

glutamine, 100 UI/ml penicillin and 100 μg/ml streptomycin (PE/ST) and amphotericin (all from Invitrogen Corporation). Culture medium of nearly confluent cell layers was replaced by 100 μl of medium containing UDL (1 and 10 mM phospholipids). Upon 1 h incubation at 37 °C, suspensions were removed; cells were washed with PBS (140 mM NaCl, 8.7 mM Na₂HPO₄, 1.8 mM NaH₂PO₄, pH 7.4) replaced by fresh RPMI medium and cells were incubated for 24 h at 37 °C. Upon incubation, supernatants were transferred to fresh tubes; centrifuged at 250 ×g for 4 min and LDH content was measured using lactate dehydrogenase CytoTox Kit (Promega) [29]. LDH concentration was expressed as percentage LDH release relative to treatment with the detergent Triton X-100 and then percentage of viability was calculated considering the LDH leakage of cells grown in medium.

2.3.2. Glutathione assay (GSH)

Total cellular glutathione of was measured using the Tietze method [30]. Culture medium of nearly confluent J774 cells was replaced by 100 μl of medium containing free ZnPc (1.25 and 12.5 μM), UDL (1 and 10 mM) UDL-ZnPc (1.25 μM ZnPc–1 mM phospholipids and 12.5 μM ZnPc–10 mM phospholipids). Upon 24 h at 37 °C incubation, suspensions were removed, replaced by fresh RPMI medium and one plate was exposed to direct sunlight along 15 min (light dose of 15 J/cm² at λ = 600–650 nm measured by Radiometer Laser Mate Q, Coherent), meanwhile other plate was kept in the dark. After treatments, cell cultures were incubated for 24 h at 37 °C, media were removed and cells were washed in PBS and collected into eppendorf tubes by trypsin treatment. Then trypsin was inactivated, cells were twice washed in PBS by centrifugation and finally suspended in 100 μl of 1 mM EDTA. Cells were lysed by sonication (tip sonicator 10 s) and cellular debris was removed by centrifugation (10000 ×g for 15 min at 4 °C). 20 μl aliquots of each supernatant were transferred to 96 wells plate for glutathione determination. The reaction was started by adding 180 μl of reaction mixture [60 μM 5,5'-dithio-bis(2-nitrobenzoic acid) (DTNB), 1.5 mM NADPH, 0.1 mM EDTA, and 2.4 U/ml GSH reductase in NaHCO₃ 0.1% (all from Sigma-Aldrich, St. Louis, MO, USA)]. Absorbance at 412 nm was monitored after 15 min with microplate reader and the glutathione concentration was determined by comparing the rate of colour change with that of a GSH standard curve.

2.4. UDL-ZnPc internalization by promastigotes

Leishmania braziliensis promastigotes (STRAIN 2903) were cultured at 25 °C in Novy–McNeal–Nicolle biphasic medium [31] and RPMI 1640 supplemented with 10% FCS and PE/ST. Before treatments, promastigotes were taken from liquid phase and transfer to RPMI medium.

L. braziliensis promastigotes were incubated with UDL-ZnPc (1.25 μM ZnPc–1 mM phospholipids) for 15 min at 4 °C and 25 °C. Upon incubation, parasites were washed by centrifugation (3830 ×g for 3 min) and fixed in 2% v/v formaldehyde in PBS. The emission of ZnPc was monitored with a confocal laser scanning microscope (CLSM) Olympus FV300 equipped with a He–Ne 633 nm laser.

2.5. Anti-promastigote activity

Promastigotes were incubated for 5 min at 25 °C with empty L and UDL (1 and 0.1 mM phospholipids) (100 μl RPMI with 10% FCS and PE/ST). Upon incubation, samples were centrifuged (3800 ×g for 10 min at 20 °C), supernatants were removed and replaced by fresh RPMI medium. Parasites were further incubated for 3 h at 25 °C and mobility was evaluated microscopically.

Promastigotes (5 × 10⁵) were incubated for 30 min at 25 °C with empty UDL (1 mM phospholipids), free ZnPc (1.25 μM), UDL-ZnPc and L-ZnPc (both 1.25 μM ZnPc–1 mM phospholipids). Upon

incubation, samples were centrifuged (3800×g for 10 min at 20 °C), supernatants were removed and replaced by fresh RPMI medium, and exposed 15 min to direct sunlight as stated before. Control cells were maintained on the dark. After treatments, parasites were incubated at for 24 h or 48 h at 25 °C and inhibition of promastigotes growth was microscopically determined by counting parasite numbers in a Neubauer haemocytometer. Anti-promastigote activity was expressed as: % APA = [1 – (no. of promastigotes treated)/(no. of promastigotes control)] × 100.

2.6. Intracellular anti-amastigote activity

RAW macrophages maintained in RPMI 1640 medium supplemented with 10% FCS and PE/ST were infected with *Leishmania* promastigotes at 1:10 macrophage: promastigotes ratio, and the following treatments were done: a. 24 h incubation with UDL-ZnPC (1.25 μM ZnPC–1 mM phospholipids) or ZnPC (1.25 μM); b. 2 h incubation with UDL-ZnPC, ZnPC or empty UDL followed by 22 h incubation in RPMI medium; c. 22 h incubation only with promastigotes followed by 2 h incubation with UDL-ZnPC or ZnPC. After incubation in the dark, suspensions were removed, replaced by fresh RPMI medium and exposed to direct sunlight along 15 min as described above. Control cells were maintained on the dark. After 24 h, the coverslips were removed, washed with PBS, fixed with methanol and stained with Giemsa. The number of amastigotes/300 cells was counted by using light microscopy. Untreated infected macrophages were used as control. Anti-amastigote activity was expressed as: % AA = [1 – (no. of amastigotes/100 cells) treated/(no. of amastigotes/100 cells) control] × 100.

2.7. In vitro skin penetration studies

Excised human skin from Caucasian female patients, who had undergone abdominal plastic surgery, was used. Patients were healthy and with no medical history of dermatological disease. After excision, the skin was cut into 10 × 10 cm² pieces and the subcutaneous fatty tissue was removed from the skin specimen using a scalpel. Afterwards the surface of each specimen was cleaned with water, wrapped in aluminum foil and stored in polyethylene bags at –26 °C until use. Previous investigations have shown that no change in the penetration characteristics occurs during the storage time of 6 months [32,33].

Disks of 24 mm in diameter were punched out from frozen skin, thawed, cleaned with PBS solution, and transferred directly into the Saarbrücken Penetration model (SPM). Briefly, the skin was put onto a filter paper soaked with Ringer solution and placed into the cavity of a Teflon block.

UDL and L containing HPTS (UDL-HPTS and L-HPTS) were prepared as stated in Section 2.2, excepting that the lipid film was hydrated with a solution containing 35 mM HPTS Tris–HCl buffer. After extrusion the free HPTS was eliminated by gel permeation chromatography in a Shepadex G-50 column using minicolumn centrifugation method [34].

UDL-HPTS or L-HPTS (11 μl/cm² corresponding to 0.12 mg phospholipids/cm² and same amount of HPTS) were applied to the skin surface, the system was placed into an oven at 35 °C, and were incubated for 1 and 5 h after drying of the vesicle solutions. Besides, UDL-ZnPC, L-ZnPC and free ZnPC solubilized in DMSO were applied to the skin disks at 2.58 nmol of ZnPC/cm², placed at 35 °C and incubated for 1 h after drying of the suspensions.

2.7.1. Skin segmentation

After incubation time the skin specimens mounted on SPM were segmented using tape stripping method or optically scanned by CLSM.

2.7.1.1. Tape stripping. After the incubation time skin specimens were segmented using tape stripping method as described by Wagner [35]. Briefly, the formulation was wiped off from the skin surface using cotton. Then the skin piece was mounted on an extruded polystyrene foam disc using small pins to stretch the tissue and covered with a teflon mask with a central hole of 15 mm in diameter for the HPTS formulations and successively stripped with 20 pieces of adhesive tape (Scotch 3 M) placed on the central hole, while for the ZnPC formulations the tapes were placed covering the whole surface of the skin segments. Each tape was charged with a weight of 2 kg per 10 s and rapidly removed.

HPTS was extracted from each tape with 3 ml of ethanol–water (1:1 v:v), shaken at 190 rpm for 1 h at 37 °C. Emission of HPTS (510 nm) was measured upon excitation at 453 nm, using a Perkin-Elmer LS 55 spectrofluorometer.

ZnPC from the twenty tapes was extracted overnight with 4 ml of DMSO at room temperature. Emission of ZnPC at 710 nm was measured upon excitation at 699 nm [36]. Calibration curves were prepared among each experiment to quantify the ZnPC, showing linear behavior between 0.01 and 0.2 μmol/l with a correlation coefficient (r²) of 0.999.

After the tape stripping, the remaining skin below the stratum corneum (SC) – i.e. the viable epidermis and the dermis – was cut into small pieces, placed into 4 ml of DMSO, homogenized, sonicated for 20 min, filtered and the fluorescence was measured the same as for the tapes [36].

2.7.1.2. Optical scanning. After incubation, the full skin thickness was optically scanned at 2 μm increments through the z-axis by CLSM equipped with an Ar laser (488 nm). Fluorescence intensity of each image was obtained by Image-J software.

2.7.2. Skin cryosectioning

UDL and L containing HPTS and Rh-PE or ZnPC (UDL-HPTS-Rh-PE/ZnPC and L-HPTS-Rh-PE/ZnPC) were prepared as stated in Section 2.2, excepting that Rh-PE (1: 1000, Rh-PE: SPC, mol:mol) or ZnPC were co-solubilized in organic solution with lipids. UDL containing Quantum Dots (UDL-QD) were prepared by hydration the thin lipid film with a suspension of 0.01 nmol QD/ml in Tris buffer. Negative staining electron microscopy images of liposomes upon uranyl acetate staining were obtained with a JEOL JEM 1200 EX II microscope.

Formulations were applied to the skin surface and incubated for 1 h in a SPM as stated before (Section 2.7). After incubation the skin was rapidly frozen in dry ice, embedded in OCT and sliced in sections of 8 μm thickness, perpendicular to the skin, with a cryomicrotome Reichert-Jung CryoCut 1800 (Germany). Skin slices were fixed with 10% formaldehyde and observed by CLSM equipped with an Ar laser (488 nm for HPTS and QD excitation) and a He–Ne laser (543 nm for Rh-PE and ZnPC excitation).

The same specimens were also subjected to hematoxylin and eosin staining in order to detect using light microscopy the possible presence of histological alterations in the analyzed tissues.

2.8. Statistical analysis

The significance of the differences between the mean values of studied parameters was determined using the Student's *t*-test.

3. Results

3.1. Size and z potential

The preparations rendered UDL-ZnPC (58 nmol ZnPC/52 μmol phospholipid/ml) of 99.9 ± 1.2 nm in size with unimodal distribution and a Zeta potential of –36.7 ± 3.8. Similar results were obtained for L-ZnPC (44 nmol ZnPC/44 μmol phospholipid/ml).

319 3.2. Cytotoxicity on mammal cells

320 The effect of empty UDL on cell membrane integrity of fibroblasts
 321 (Vero cells) and of macrophages (J-774 cells) was determined by LDH
 322 leakage. UDL at 1 mM phospholipids did not induce LDH leakage on
 323 both cell types, although at 10 mM caused 80% leakage of LDH on J774
 324 cells upon 1 h incubation (Fig. 1a). L did not produce LDH leakage
 325 either at 1 or 10 mM (data not shown). Additionally, total GSH level in
 326 J774 cells was measured upon incubation with UDL-ZnPc followed by
 327 sun irradiation. GSH level was not altered after incubation with free
 328 ZnPc, empty UDL and UDL-ZnPc (1 mM phospholipids–1.25 μ M ZnPc)
 329 in the dark or after irradiation. Although, GSH was significantly
 330 diminished upon incubation at 10 mM phospholipids–12.5 μ M ZnPc
 331 followed by 15 min of sun irradiation (Fig. 1b). 12.5 μ M free ZnPc and
 332 10 mM empty UDL did not affected GHS level.

333 3.3. UDL-ZnPc internalization by promastigotes

334 *L. braziliensis* promastigotes were incubated with UDL-ZnPc at
 335 25 °C (optimum temperature of growth) and at 4 °C (temperature at
 336 which internalization by endocytic uptake is absent due to reduced
 337 metabolism of cells [37]) to distinguish between active uptake and
 338 superficial adsorption. Fluorescence microscopy showed higher
 339 intensity of fluorescence upon incubation at 25 °C than at 4 °C
 340 (Fig. 2). These results could suggest that UDL-ZnPc were internalized
 341 by promastigotes by endocytic uptake.

342 3.4. Anti-promastigote activity

343 First, it was observed that around 17 and 29% of promastigotes lost
 344 motility upon incubation with L at 0.1 and 1 mM, respectively, while
 345 the rest of the parasites kept highly mobile. Although, 5 min
 346 incubation with UDL induced an important diminish of motility. 90%
 347 of parasites lost motility after incubation with UDL at 0.1 and 1 mM,

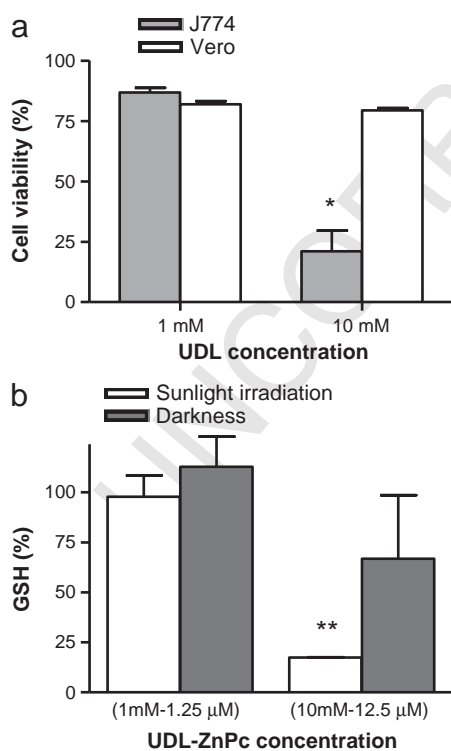


Fig. 1. Mammal cells cytotoxicity measured as LDH leakage induced by UDL on J774 and Vero cells upon 1 h incubation (a) and GSH content in J774 cells after incubation with UDL-ZnPc in the dark or upon irradiation (b). Each data point represents the mean \pm standard deviation ($n=3$). * $p<0.05$, ** $p<0.01$.

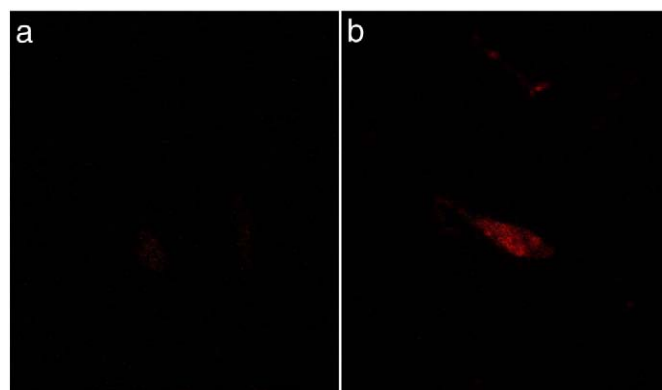


Fig. 2. CLSM images of *L. braziliensis* promastigotes incubated with UDL-ZnPc at 4 °C (a) and 25 °C (b).

meanwhile the rest of the parasites kept highly mobile (0.1 mM) or 348
 with low motility (1 mM). 349

Then, to determine if lost of motility were related with loss of 350
 viability, anti-promastigote activity (APA) was determined after 351
 30 min incubation followed by 24 or 48 h of parasite growth. First, 352
 empty UDL and UDL-ZnPc in the dark showed high and similar APA of 353
 around 80% after 24 h of growth. Nevertheless, the highest anti- 354
 promastigote effect (100% APA) was shown upon 15 min of sun 355
 irradiation of promastigotes treated with UDL-ZnPc (Fig. 3). Upon 356
 48 h of parasite growth, the all the treatments showed APA of around 357
 100%. 358

On the other hand, free ZnPc at 1.25 μ M did not affect the motility 359
 of promastigotes upon 5 min incubation and it showed a 20% APA 360
 after sun irradiation and 48 h of parasite growth, while L-ZnPc 361
 showed 0% APA in the darkness or upon irradiation (data not shown). 362

363 3.5. Intracellular anti-amastigote activity

Anti-amastigote activity (AA) was determined in two ways: first, 364
 samples were co-incubated for 2 or 24 h with RAW macrophages and 365
 promastigotes and second, samples were incubated for 2 h with 366
 macrophages previously infected. 367

Empty UDL had insignificant AA (5%), meanwhile activity of free 368
 ZnPc and UDL-ZnPc increased as time of incubation increased from 2 369
 to 24 h (Fig. 4a). While free ZnPc showed activity only upon 370
 irradiation (20 and 35% AA after 2 and 24 h, respectively), when 371
 incorporated in UDL (UDL-ZnPc) activities in the dark or upon 372
 irradiation were not different (AA 40 and 80% after 2 and 24 h, 373
 respectively), but were almost the double of AA for free ZnPc. 374

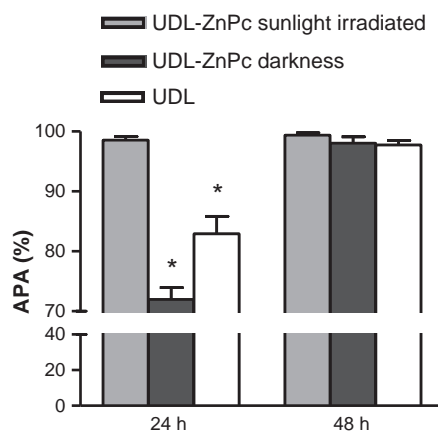


Fig. 3. Anti-promastigote activity (APA%) of UDL and UDL-ZnPc in the dark or upon 15 min sunlight irradiation. * $p<0.05$.

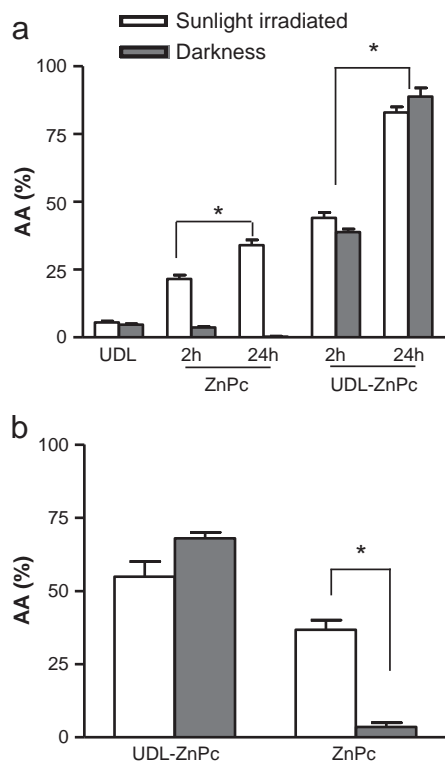


Fig. 4. Anti-amastigote activity (AA%) of UDL, ZnPc and UDL-ZnPc co-incubated with RAW macrophages and *L. braziliensis* promastigotes for 2 or 24 h (a), and of UDL-ZnPc and ZnPc incubated with RAW macrophages previously infected with *L. braziliensis* promastigotes for 2 h (b). Cells were then exposed to 15 min sunlight irradiation or maintained in the dark and grown for 24 h. * $p < 0.05$.

375 Finally, free ZnPc as well as UDL-ZnPc showed AA upon 2 h
376 incubation with infected macrophages (Fig. 4b). Again, free ZnPc
377 activity was irradiation dependent (3 vs 36% AA, in the dark and after
378 irradiation, respectively), while UDL-ZnPc activity was independent
379 (55% AA) and higher than AA for free ZnPc.

380 3.6. *In vitro* skin penetration studies

381 Skin penetration of the hydrosoluble fluorescent dye HPTS
382 encapsulated in UDL and L was determined using the SPM followed
383 by segmentation by tape stripping or optical scanning by CLSM up to
384 60 μm depth. The presence of ZnPc in SC and in deeper viable
385 epidermis and dermis upon incubation as free ZnPc, UDL-ZnPc and L-
386 ZnPc was also quantified. Finally, skin penetration of HPTS and the
387 hydrophobic Rh-PE or ZnPc co-encapsulated in UDL and L were
388 recorded by cryosectioning to assess the integrity of vesicles along
389 penetration.

390 SPM was employed under non-occlusive conditions, in order to
391 maintain the humidity gradient across the skin, that it is proposed to
392 be the locomotive force for UDL penetration [38]. If compared with
393 Franz diffusion cell, SPM avoids the non-physiological hydration and
394 changes of the skin due to the absence of liquid as receptor medium.
395 This system, coupled to segmentation techniques, such as tape
396 stripping or cryosectioning, allows the measurement of penetration
397 profiles of drugs with respect to the depth of the tissue. To avoid the
398 reported variability of the tape stripping [39–41], the experiments
399 were carried out with the same skin donor, repeated 5 times and the
400 distance and geometry of skin fixation – responsible for maintaining
401 the stretching of the skin during tape stripping – were kept constant.

402 Fluorescence profiles of UDL-HPTS and L-HPTS extracted from
403 each strip upon 1 h incubation were significantly different (Fig. 5).
404 The cumulative of fluorescence in the 20 strips (corresponding to the
405 total SC), was around 6.8 folds higher for UDL-HPTS than for L-HPTS

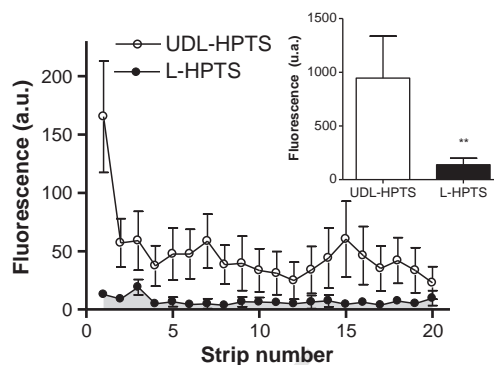


Fig. 5. SC strip profile of HPTS after 1 h of non-occlusive application of UDL-HPTS or L-HPTS ($n = 5$). Inset: Cumulative fluorescence in the 20 strips. ** $p < 0.01$.

(Inset Fig. 5). Fluorescence profiles and accumulated fluorescence 406
upon 5 h incubation were similar to those obtained after 1 h of 407
incubation, for both formulations. 408

In this procedure, each removed cell layer had nearly the same 409
thickness [35,42] being the number of tape strips linearly correlated 410
with the remaining thickness of the SC. According to this, UDL-HPTS 411
penetrated deeper into the SC than L-HPTS. 412

The optical scanning (Fig. 6) showed that HPTS distributed in SC 413
layers in patterns similar, but slightly thicker than the net of 414
nanochannels previously described [43,44]. 415

The use of SPM ensured that the detected fluorescence was 416
exclusively owed to the penetration of HPTS, Rh-PE or ZnPc from top 417
to bottom at the lower layers of the epidermis, and not to the 418
basolateral penetration which is inherent to the Franz cell [35]. 419

Transversal skin cryosections after 1 h incubation with double 420
fluorescently labeled liposomes (UDL-HPTS-Rh-PE/ZnPc or L-HPTS- 421
Rh-PE/ZnPc), showed maximal fluorescence intensity of Rh-PE/ZnPc 422
from UDL at the first 8 μm up to a depth of 14 μm , in the boundaries of 423
the viable epidermis (8–13 μm [45]). Based on the osmotic force 424
theory of Cevc and Blume [46], the UDL would not penetrate beyond 425
the non-hydrated deepest layers of the SC. The hydrophilic HPTS 426

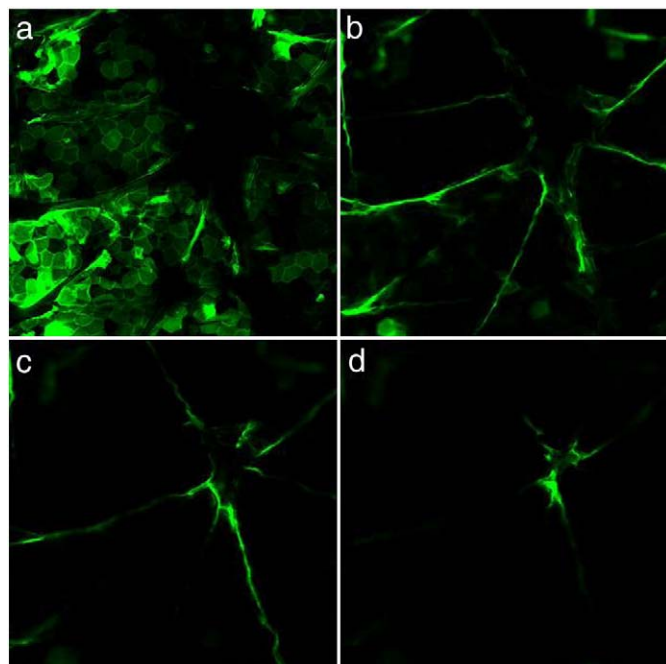


Fig. 6. Typical series of CLSM images obtained horizontally at 0 μm (a), 20 μm (b), 40 μm (c) and 60 μm (d) from skin surface upon 1 h incubation with UDL-HPTS.

427 however, was found in a separate fraction, entering the viable
428 epidermis, up to a mean depth of 24 μm (Fig. 7a and b). On the
429 contrary, fluorescence of Rh-PE/ZnPc from L was only detected at
430 the first 1 μm (first SC cells layer), while a slight diffuse poorly intense
431 fluorescence from HPTS was found up to 2 μm (Fig. 7c and d).

432 After 1 h incubation in SPM of 11.7 nmol ZnPc (dissolved in
433 DMSO at 0.98 $\mu\text{mol}/\text{ml}$)/4.5 cm^2 total area, followed by removal of
434 material remaining on the skin surface, it was found that only 1 out
435 of 5 skin samples contained ZnPc in quantitative amounts within SC,
436 viable epidermis and dermis (data not shown). On the contrary,
437 upon applying the same amount of ZnPc/4.5 cm^2 either as UDL-ZnPc
438 or L-ZnPc, it was found that UDL-ZnPc delivered 7.35 folds higher
439 amount of ZnPc than L-ZnPc. As judged by the penetration profile of
440 Rh-PE/ZnPc in Fig. 7 it was reasonably to assume that the UDL-ZnPc
441 (lipid matrix and ZnPc) homogeneously distributed across the
442 $\sim 8 \mu\text{m}$ thickness of the SC, whereas L-ZnPc remained stacked on
443 the first layer of the SC. In other words, upon applying the same
444 amount ZnPc/surface, $\sim 3.8 \times 10^{-2}$ nmol UDL-ZnPc were evenly
445 distributed in a volume of [1 cm^2 surface $\times 8 \times 10^{-4}$ cm depth] of
446 SC, while $\sim 5.4 \times 10^{-3}$ nmol L-ZnPc distributed in a volume of [1 cm^2
447 surface $\times 1 \times 10^{-4}$ cm depth]. Hence, UDL-ZnPc rendered nearly 7
448 more ZnPc within the SC, distributed in a cylinder 8 fold more
449 profound than L-ZnPc. Assuming a homogeneous distribution, the
450 concentration of UDL-ZnPc within the whole depth of SC was 47 μM ,
451 far beyond the concentration that *in vitro* was necessary to kill
452 promastigotes upon 15 min sunlight irradiation. UDL-ZnPc also
453 rendered nearly 40 folds higher amount ZnPc (8.63×10^{-3} nmol)
454 distributed across the reminder viable epidermis and dermis, than L-
455 ZnPc (Fig. 8). Again, only 1 out of 5 skins showed a significant
456 presence of ZnPc within the rest of skin when it was applied in DMSO
457 solution (data not shown).

458 Finally, the penetration profile of QD and UDL-QD was determined.
459 The UDL-QD suspension was translucent with a mean vesicular size of
460 102 nm and polydispersity index of 0.128 (Fig. 9a and b). After 1 h
461 incubation, the fluorescence of QD was distributed both across the SC
462 as well across the viable epidermis (Fig. 10a) in coincidence with
463 other authors [47], whereas that of UDL-QD remained confined in the
464 thickness of the SC (Fig. 10b).

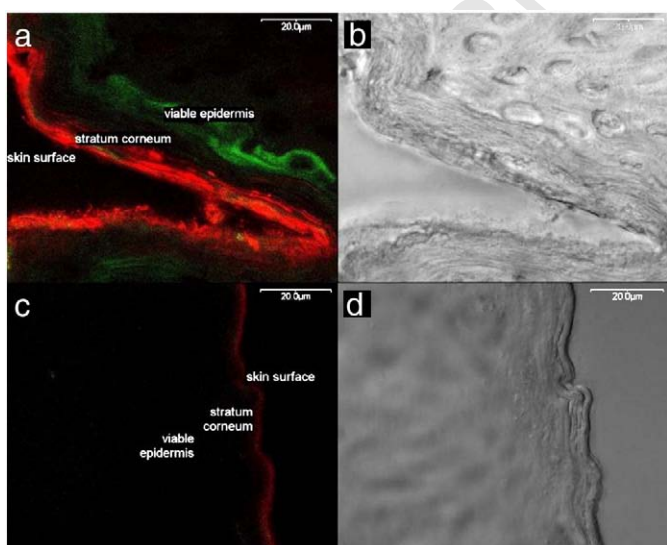


Fig. 7. CLSM images of cryosectioned skin after 1 h incubation with UDL-HPTS-rh-PE (a and b, fluorescence and the corresponding differential interference contrast image, respectively) and with L-HPTS-rh-PE (c and d, fluorescence and the corresponding differential interference contrast image, respectively). Red and green signals from rh-PE and HPTS, respectively. (For interpretation of the references to colour in this figure legend, the reader is referred to the web version of this article).

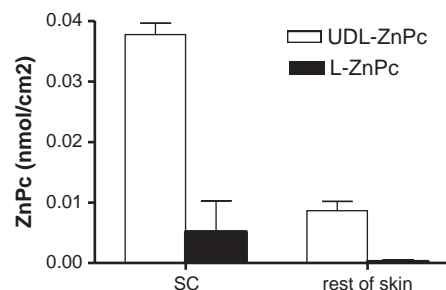


Fig. 8. Penetration of ZnPc in skin layers after 1 h non-occlusive incubation with UDL-ZnPc and L-ZnPc.

4. Discussion

465

466 *In vitro*, aminolevulinic acid (ALA)-PDT fails in eliminate the
467 intracellular leishmania amastigotes. For instance, 4 h incubation with
468 ALA follow by irradiation with a 635 nm laser up to 50 J/cm^2 of *L major*
469 infected J774 cells, reduce the number of J774 cells but does not
470 diminish the number of intracellular parasites [48]. The reason for this
471 is that only mammal host cells can metabolize the ALA precursor to
472 the photosensitizer protoporphyrin IX (PpIX). PpIX is further
473 accumulated inside the intracellular amastigotes in an amount
474 insufficient to kill the parasites at fluence of 10 J/cm^2 . The phototoxic
475 effect against parasites occurs at a high concentration of PpIX
476 ($\text{LD}_{50} \approx 3.8 \times 10^{-4}$ M), that cannot be applied *in vivo* without
477 generating serious toxic side effects. Clinically however, succeed
478 application of ALA- and MAL-PDT to CL patients caused by *L. donovani*
479 and *L major*, have been published in 2003 and 2004 [49–51]. Recently,
480 it was shown that lesions healed rapidly with good cosmetics in a
481 patient with facial cutaneous *L. tropica* infection resistant to various
482 therapeutic regimens after MAL-PDT treatment [23] and improved
483 results were found in a comparative study between ALA-PDT and
484 topical paromomycin [52]. It is feasible that *in vivo* the induction of a
485 local immune response (for instance increased levels of IL-6) leading
486 to a non-specific tissue damage accompanied by macrophages
487 elimination, should account for the success of the ALA-PDT [48]. In
488 other words, the leishmanicidal effect is mediated by an immune host
489 reaction against a non-specific photochemical damage, and not by a
490 selective effect exclusively elicited by the PDT.

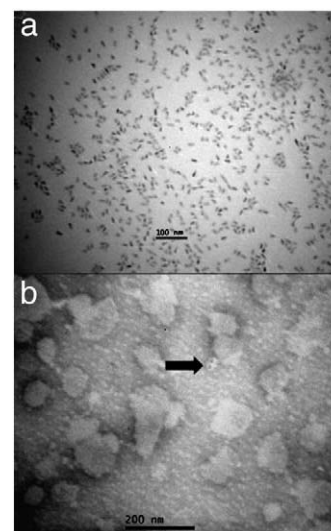


Fig. 9. Transmission electron microscopy images of free QD (a) (ellipsoidal shape, 6 nm short axis, 12 nm long axis and hydrodynamic diameter due to polyethylene glycol coverage up to 45 nm [68]) and UDL-QD (b). Arrow points to QD contained inside UDL.

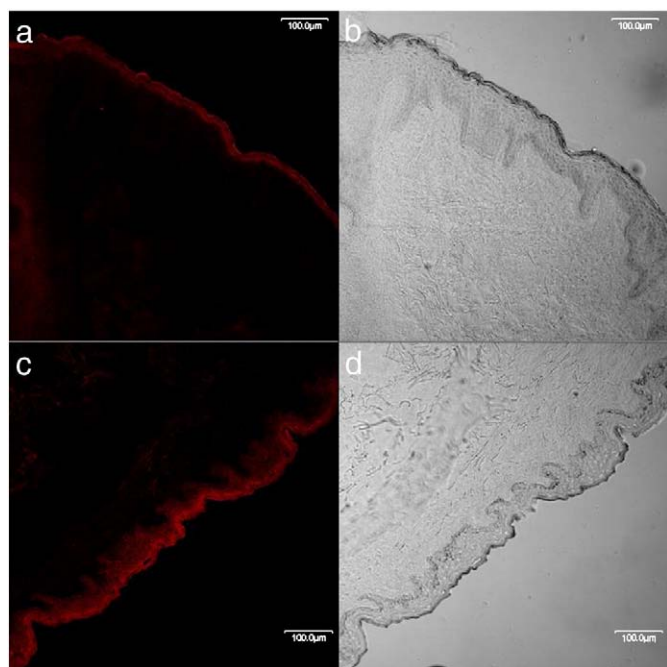


Fig. 10. CLSM images of cryosectioned skin after 1 h of incubation with UDL-QD (a and b, fluorescence and the corresponding differential interference contrast image, respectively) and with QD (c and d, fluorescence and the corresponding differential interference contrast image, respectively).

491 Different photosensitizers such as phenothiazinium, aluminum
492 chloride phthalocyanine and zinc phthalocyanine (with direct action
493 in their intact form), also have shown succeeding preclinical results in
494 the last four years [53,54]. In particular, results from Dutta indicates
495 that promastigotes and axenic amastigotes of *L. amazonensis* are more
496 sensitive than J774 macrophages to light mediated cytolysis at low
497 concentration (1 μM) of the hydrophobic aluminum phthalocyanine
498 chloride (AlPhCl) under a low energy dose (1.5 J/cm^2). Nevertheless,
499 AlPhCl had no AA on infected J774 cells, and intracellular amastigotes
500 could be eliminated only when AlPhCl was previously incubated with
501 axenic amastigotes before the macrophages were infected [55]. This
502 fact suggested that the cell membrane could hinder the free access of
503 AlPhCl to intracellular targets.

504 A suitable delivery system could help to overcome the tissue and
505 cellular barriers interposed between hydrophobic phthalocyanines
506 and target amastigotes. Actually, the co-localization of phthalocyanine
507 and target in a small volume of space should be the key to optimize
508 the photodynamic activity, because of the short half life (<0.1 ms) and
509 small action radii (10–20 nm) of singlet oxygen [56]. However,
510 changing both the internalization mechanism and the intracellular
511 traffic of the phthalocyanine (free phthalocyanine diffuse across the
512 plasma membrane, and then relocate to other intracellular mem-
513 branes [57]) by means of a delivery system could also arise
514 unexpected toxic effects.

515 With the aim of improving the penetration of the hydrophobic
516 ZnPc across the intact SC without using organic solvents and to count
517 on a particulate vehicle with increased chances of being selectively
518 captured by infected macrophages in the skin, we had previously
519 characterized and determined the photochemical parameters of ZnPc
520 loaded in a highly hydrophilic ultradeformable lipid matrix. When
521 partitioned in UDL bilayers, ZnPc remains in monomeric form and
522 exhibit similar photodynamic properties than in organic solvents, as
523 judged by the similar value of the singlet oxygen quantum yield from
524 UDL-ZnPc and ZnPc in ethanol. Upon UDL-ZnPc internalization, the
525 phago/lysosomal compartment of macrophages remains intact after
526 15 min of sunlight irradiation. Cytotoxicity, as measured by the MTT
527 assay on Vero and J774 cells, is absent up to 10 μM free ZnPc, as well as

for up to 18 mM empty UDL, both in the dark or after 15 min sunlight
irradiation. UDL-ZnPc at 10 μM ZnPc–8 mM phospholipids however,
reduces 75% J774 cell viability, not only after irradiation but also in the
dark [27].

528
529
530
531
532 In this work the GSH levels and release of cytosolic LDH were
533 tested to delimit a safe threshold concentration of UDL and UDL-ZnPc
534 when incubated with host phagocytes. The crucial factors determin-
535 ing the type of cell death following PDT are cell type, the subcellular
536 localization of the photosensitizer, and the light dose applied [58]
537 (lower doses – such as the one received upon 15 min sunlight
538 irradiation – lead to more apoptotic cells, while higher doses result in
539 more necrotic cells [59]). Diminished GSH (the principal intracellular
540 low-molecular-weight thiol that plays a critical role in the cellular
541 defence against oxidative and nitrosative stress in mammalian cells)
542 levels are observed in the early stages of apoptosis [60]. We found that
543 1.25 μM free ZnPc or as UDL-ZnPc and 1 mM phospholipids empty
544 UDL did not diminish the intracellular GSH level in J774 cells, neither
545 in the darkness nor after 15 min sunlight irradiation. The presence of
546 30 mol% of the detergent sodium cholate within the UDL matrix could
547 induce membrane damages when in contact to host cell surface, but
548 1 mM phospholipids empty UDL did not induce the release of LDH
549 neither by Vero nor J774 cells. At 10 mM however, an important
550 release of LDH was produced by J774 cells, which was absent at the
551 same concentration of L phospholipids. The faster uptake rate of
552 phagocytosis, leading to higher amounts of internalized detergent in
553 comparison to endocytosis [61], could be the reason for this non-
554 photodynamic damage caused by UDL on J774.

555 The leishmanicidal activity was tested at 1 mM phospholipids
556 and 1.25 μM ZnPc upon 15 min sunlight irradiation since neither
557 photodynamic nor non-photodynamic damage as measured by MTT,
558 LDH assays and GSH consumption by phagocytic cells was registered
559 below these threshold concentrations. Only 5 min incubation at
560 25 $^{\circ}\text{C}$ was sufficient for empty UDL to produce an important decrease
561 in motility of promastigotes. Same sized L neither caused relevant
562 effect on parasite motility nor was captured by promastigotes, in
563 accordance with previous results indicating that submicron diam-
564 eter L can only be absorbed on the surface of cell parasites [62]. The
565 intense fluorescence signal from UDL-ZnPc associated to the parasite
566 upon 15 min incubation at 25 $^{\circ}\text{C}$ suggested an active uptake of UDL.
567 The cytoskeleton of *Leishmania* promastigote is organized as a
568 microtubule network underlying the cell membrane. The only
569 available area for exchange of macromolecules with the external
570 environment is the nearly 1 μm^2 surface of the flagellar pocket
571 [63,64]. The elastic modulus of UDL is twenty folds lower than that of
572 L, allowing for micro/nanoscaled spontaneous fluctuations of the
573 bilayer at room temperature [65]. This could facilitate its endocytic
574 uptake by the flagellar pocket. Hence the lipid matrix ultradeform-
575 ability leading to its internalization and parasite immobilization
576 could be the source of the observed non-photodynamic leishmanicidal
577 activity.

578 On the other hand, UDL-ZnPc showed 100% APA (five folds
579 increased over that of free ZnPc) after 15 min sunlight irradiation.
580 Both UDL-ZnPc in the darkness as well as empty UDL also exhibited
581 around 80% APA, while ZnPc and L-ZnPc did not (this last even after
582 sunlight irradiation). These facts indicated that a high APA could
583 simply be induced by internalization of empty ultradeformable
584 matrices. For UDL-ZnPc, the irradiation yet contributed to accelerate
585 the leishmanicidal effect upon internalization.

586 As UDL-ZnPc, AA raised up to 80% (more than two folds increased
587 over that of the strictly sunlight dependent AA of free ZnPc) when co-
588 incubated with promastigotes and RAW macrophages along 24.
589 Remarkably, AA of UDL-ZnPc was independent of irradiation. Part of
590 the 80% AA could arise from APA caused by UDL/UDL-ZnPc before
591 infecting the RAW cells. In other words, probably the observed AA
592 aroused from an infection occurred with a lower amount of viable
593 parasites that the stated in the experimental method.

Taken together, though formerly aimed for PDT, these results indicated that an important part of the UDL-ZnPc leishmanicidal activity was independent of the irradiation. As previously discussed, the empty ultradeformable lipid matrix was an effective non-photodynamic leishmanicidal agent that fully manifested as *in vitro* APA. The *in vitro* AA of UDL was absent, but the non-photodynamic AA from UDL-ZnPc was unexpectedly high. And explanation for this could be that phagocytosis of UDL-ZnPc by host cells resulted in products that were innocuous for the host but lethal for the parasites.

As previously observed by Cevc [38] and Honeywell–Nguyen [44], we determined that the hydrophobic Rh-PE or ZnPc and the hydrophilic HPTS when loaded in UDL rapidly entered the SC, but did not if loaded in L. Also in accordance to Honeywell–Nguyen [40,66] who determined that a hydrophilic drug is released from the lipid matrix diffusing to deeper layers in the epidermis, the hydrophobic molecules Rh-PE/ZnPc were found at the SC-viable epidermal junction, while HPTS was found deeper in the epidermis. At the end of the SC, the hydrophilic molecules were shuttled from the carrier.

Our results indicated that UDL-ZnPc penetrated homogeneously in the SC, carrying 7 folds higher amount of ZnPc 8 folds deeper than L-ZnPc while ZnPc in DMSO did it in a poorly reproducible fashion after 1 h incubation. Three weeks is the elapsed time for desquamation and renewal of SC [67] and probably within that period the UDL-ZnPc concentrated in SC would act as a reservoir for delivery of lipid matrix and ZnPc to the viable epidermis. Remarkably, the UDL-ZnPc was the only formulation ensuring a reproducible and quantitative delivery of ZnPc to the viable epidermis and dermis upon a single application and 1 h incubation. This amount could be increased after multiple applications. Infected macrophages can be found at different levels within the viable epidermis and clearly UDL-ZnPc showed to be a suitable tool to increase the amount of ZnPc delivered into and beyond the SC, as judged by this *in vitro* assay.

Infected macrophages are specialized in the uptake of particulate material. Hence the chances of being internalized should be increased as long as the vesicular integrity of UDL-ZnPc is conserved. Since the high sized ellipsoidal QD remained trapped into the relatively small (100 nm diameter) UDL matrix, probably the vesicular structure of the UDL were conserved along the SC penetration. Otherwise the QD should squeeze deeper into the epidermis, as the free QD did. Hence, excluding the use of organic solvents such as dimethylsulphoxide or dimethylformamide that are required to dissolve highly hydrophobic molecules like ZnPc, we could reasonably expect that in spite of the loss of hydrophilic content across the SC penetration, the ZnPc-UDL could get close to the viable epidermis in an – at least – partly particulate form.

Further studies will reveal if these UDL when applied in minimal doses on the surface of intact skin could have a preventive or therapeutic effect aroused both from their photodynamic activity as well as from their non-photodynamic activity during the first stages of the infection. It is likely that the leishmanicidal effect upon transcutaneous application of UDL could result from a synergistic effect fruit from its multiple leishmanicidal activity and its superior capacity of penetration.

Acknowledgements

This work was supported by a grant from the Secretaria de Investigaciones, Universidad Nacional de Quilmes, and from the Comisión de Investigaciones Científicas de la Provincia de Buenos Aires. MJ Morilla and EL Romero are members of the Carrera del Investigador Científico del Consejo Nacional de Investigaciones Científicas y Técnicas, Argentina (CONICET). J. Montanari has got a fellowship from CONICET. Dr H Jimenez provided the skin explants from surgery. Students LA Lado and L Rivadeneira collaborated in the development of the skin experiments.

References

- R. Bonfante, S. Barruela, Leishmaniasis y Leishmaniasis en América con especial referencia a Venezuela, Tipografía y Litografía Horizonte C.A., Caracas, 2002.
- S. Jeronimo, A. de Queiroz Sousa, R. Pearson, in: R. Guerrant, D. Walker, P. Weller (Eds.), Tropical Infectious Diseases: Principles, Pathogens and Practice, Churchill Livingstone Elsevier, Edinburgh, Scotland, 2006, pp. 1095–1113.
- B.L. Herwaldt, Leishmaniasis, Lancet 354 (9185) (1999) 1191–1199.
- WHO, Leishmaniasis, 2004.
- C.R. Davies, E.A. Llanos-Cuentas, S.J. Sharp, J. Canales, E. Leon, E. Alvarez, N. Roncal, C. Dye, Cutaneous leishmaniasis in the Peruvian Andes: factors associated with variability in clinical symptoms, response to treatment, and parasite isolation rate, Clin. Infect. Dis. 25 (2) (1997) 302–310.
- C. Bern, J.H. Maguire, J. Alvar, Complexities of assessing the disease burden attributable to leishmaniasis, PLoS Negl. Trop. Dis. 2 (10) (2008) e313.
- E. Schwartz, C. Hatz, J. Blum, New world cutaneous leishmaniasis in travellers, Lancet Infect. Dis. 6 (6) (2006) 342–349.
- S.D. Lawn, J. Whetham, P.L. Chiodini, J. Kanagalilingam, J. Watson, R.H. Behrens, D.N. Lockwood, New world mucosal and cutaneous leishmaniasis: an emerging health problem among British travellers, QJM 97 (12) (2004) 781–788.
- D. Campbell-Lendrum, J.P. Dujardin, E. Martinez, M.D. Feliciangeli, J.E. Perez, L.N. Silans, P. Desjeux, Domestic and peridomestic transmission of American cutaneous leishmaniasis: changing epidemiological patterns present new control opportunities, Mem. Inst. Oswaldo Cruz 96 (2) (2001) 159–162.
- J.A. Patz, T.K. Graczyk, N. Geller, A.Y. Vittor, Effects of environmental change on emerging parasitic diseases, Int. J. Parasitol. 30 (12–13) (2000) 1395–1405.
- P. Desjeux, Leishmaniasis: current situation and new perspectives, Comp. Immunol. Microbiol. Infect. Dis. 27 (5) (2004) 305–318.
- J. Blum, P. Desjeux, E. Schwartz, B. Beck, C. Hatz, Treatment of cutaneous leishmaniasis among travellers, J. Antimicrob. Chemother. 53 (2) (2004) 158–166.
- R.D. Pearson, S.M.B. Jeronimo, A.Q. Sousa, in: S.H. Gillespie, R. D. P. (Org.) (Eds.), Principles and Practice of Clinical Parasitology, Vol. 1, John Wiley & Sons, Chichester, 2001, pp. 287–313.
- L. Sanchez-Saldana, Leishmaniasis, Dermatol. Peru 14 (2) (2004) 82–98.
- J. Ampuero Vela, Leishmaniasis, Ministerio de Salud, Lima, Peru, 2000.
- F. Modabber, P.A. Buffet, E. Torreele, G. Milon, S.L. Croft, Consultative meeting to develop a strategy for treatment of cutaneous leishmaniasis. Institute Pasteur, Paris. 13–15 June, 2006, Kinetoplastid Biol. Dis. 6 (2007) 3.
- P. Minodier, P. Parola, Cutaneous leishmaniasis treatment, Travel Med. Infect. Dis. 5 (3) (2007) 150–158.
- D. Vardy, Y. Barenholz, N. Naftoliev, S. Klaus, L. Gilead, S. Frankenburg, Efficacious topical treatment for human cutaneous leishmaniasis with ethanolic lipid amphotericin B, Trans. R. Soc. Trop. Med. Hyg. 95 (2) (2001) 184–186.
- A. Zvulunov, E. Cagnano, S. Frankenburg, Y. Barenholz, D. Vardy, Topical treatment of persistent cutaneous leishmaniasis with ethanolic lipid amphotericin B, Pediatr. Infect. Dis. J. 22 (6) (2003) 567–569.
- T. Hasan, B. Ortel, N. Solban, B. Pogue, in: B.R. Kufe DW, W.N. Hait, W.K. Hong, R. Pollock, R.R. Weichselbaum, H.J. Gansler T, E. Frei III (Eds.), Cancer Medicine, BC Decker Inc., Hamilton, Ontario, Canada, 2006, pp. 537–548.
- Y. Nitzan, H.M. Wexler, S.M. Finegold, Inactivation of anaerobic bacteria by various photosensitized porphyrins or by hemin, Curr. Microbiol. 29 (3) (1994) 125–131.
- P.G. Calzavara-Pinton, M. Venturini, R. Sala, A comprehensive overview of photodynamic therapy in the treatment of superficial fungal infections of the skin, J. Photochem. Photobiol. B 78 (1) (2005) 1–6.
- S. Sohl, F. Kauer, U. Paasch, J.C. Simon, Photodynamic treatment of cutaneous leishmaniasis, J. Dtsch Dermatol. Ges. 5 (2) (2007) 128–130.
- K. Pizinger, P. Cetkovska, D. Kacerovska, M. Kumpova, Successful treatment of cutaneous leishmaniasis by photodynamic therapy and cryotherapy, Eur. J. Dermatol. 19 (2) (2009) 172–173.
- E.M. van der Snoek, D.J. Robinson, J.J. van Hellemond, H.A. Neumann, A review of photodynamic therapy in cutaneous leishmaniasis, J. Eur. Acad. Dermatol. Venereol. 22 (8) (2008) 918–922.
- N.I.H. NIH Clinical Trials ID: NCT00840359, Study of the Efficacy of Daylight Activated Photodynamic Therapy in the Treatment of Cutaneous Leishmaniasis, Hadassah Medical Organization, vol. 2009, 2009.
- J. Montanari, A.P. Perez, F. Di Salvo, V. Diz, R. Barnadas, L. Dicelio, F. Doctorovich, M.J. Morilla, E.L. Romero, Photodynamic ultradeformable liposomes: design and characterization, Int. J. Pharm. 330 (1–2) (2007) 183–194.
- C.J.F. Bötcher, C.M. Van Gent, C. Pries, A rapid and sensitive submicro phosphorus determination, Anal. Chim. Acta 24 (1961) 203–204.
- C. Korzeniewski, D.M. Callewaert, An enzyme-release assay for natural cytotoxicity, J. Immunol. Meth. 64 (3) (1983) 313–320.
- F. Tietze, Enzymic method for quantitative determination of nanogram amounts of total and oxidized glutathione: applications to mammalian blood and other tissues, Anal. Biochem. 27 (3) (1969) 502–522.
- B.C. Walton, J.J. Shaw, R. Lainson, Observations on the *in vitro* cultivation of Leishmania braziliensis, J. Parasitol. 63 (6) (1977) 1118–1119.
- S.M. Harrison, B.W. Barry, P.H. Dugard, Effects of freezing on human skin permeability, J. Pharm. Pharmacol. 36 (4) (1984) 261–262.
- U. Schaefer, H. Loth, An *ex vivo* model for the study of drug penetration into human skin, Pharm. Res. 13 (1996) 66.
- D.W. Fry, J.C. White, I.D. Goldman, Rapid separation of low molecular weight solutes from liposomes without dilution, Anal. Biochem. 90 (2) (1978) 809–815.
- H. Wagner, K.H. Kostka, C.M. Lehr, U.F. Schaefer, Drug distribution in human skin using two different *in vitro* test systems: comparison with *in vivo* data, Pharm. Res. 17 (12) (2000) 1475–1481.

- 743 [36] F.L. Primo, M.M.A. Rodrigues, A.R. Simioni, M.V.L.B. Bentley, P.C. Morais, A.C.
744 Tedesco, In vitro studies of cutaneous retention of magnetic nanoemulsion loaded
745 with zinc phthalocyanine for synergic use in skin cancer treatment, *J. Magn. Magn.*
746 *Mater.* 320 (2008) e211–e214.
- 747 [37] K.A. Mullin, B.J. Foth, S.C. Ilgoutz, J.M. Callaghan, J.L. Zawadzki, G.I. McFadden, M.J.
748 McConville, Regulated degradation of an endoplasmic reticulum membrane
749 protein in a tubular lysosome in *Leishmania mexicana*, *Mol. Biol. Cell* 12 (8)
750 (2001) 2364–2377.
- 751 [38] G. Cevc, A. Schatzlein, H. Richardsen, Ultra-deformable lipid vesicles can penetrate
752 the skin and other semi-permeable barriers unfragmented. Evidence from double
753 label CLSM experiments and direct size measurements, *Biochim. Biophys. Acta*
754 1564 (1) (2002) 21–30.
- 755 [39] P.L. Honeywell-Nguyen, H.W. Wouter Groenink, A.M. de Graaff, J.A. Bouwstra, The
756 in vivo transport of elastic vesicles into human skin: effects of occlusion, volume
757 and duration of application, *J. Control. Release* 90 (2) (2003) 243–255.
- 758 [40] P.L. Honeywell-Nguyen, G.S. Gooris, J.A. Bouwstra, Quantitative assessment of the
759 transport of elastic and rigid vesicle components and a model drug from these
760 vesicle formulations into human skin in vivo, *J. Invest. Dermatol.* 123 (5) (2004)
761 902–910.
- 762 [41] A. Henning, U.F. Schaefer, D. Neumann, Potential pitfalls in skin permeation
763 experiments: influence of experimental factors and subsequent data evaluation,
764 *Eur. J. Pharm. Biopharm.* 72 (2) (2009) 324–331.
- 765 [42] J.-C. Tsai, M.J. Cappel, N.D. Weiner, G.L. Flynn, J.J. Ferry, Solvent effects on the
766 harvesting of stratum corneum from hairless mouse skin through adhesive tape
767 stripping in vitro, *Int. J. Pharm.* 68 (1–3) (1991) 127–133.
- 768 [43] B.A. van den Bergh, J.A. Bouwstra, H.E. Junginger, P.W. Wertz, Elasticity of vesicles
769 affects hairless mouse skin structure and permeability, *J. Control. Release* 62 (3)
770 (1999) 367–379.
- 771 [44] P.L. Honeywell-Nguyen, A.M. de Graaff, H.W. Groenink, J.A. Bouwstra, The in vivo
772 and in vitro interactions of elastic and rigid vesicles with human skin, *Biochim.*
773 *Biophys. Acta* 1573 (2) (2002) 130–140.
- 774 [45] K.A. Holbrook, G.F. Odland, Regional differences in the thickness (cell layers) of
775 the human stratum corneum: an ultrastructural analysis, *J. Invest. Dermatol.* 62
776 (4) (1974) 415–422.
- 777 [46] G. Cevc, G. Blume, Lipid vesicles penetrate into intact skin owing to the
778 transdermal osmotic gradients and hydration force, *Biochim. Biophys. Acta*
779 1104 (1) (1992) 226–232.
- 780 [47] J.P. Ryman-Rasmussen, J.E. Riviere, N.A. Monteiro-Riviere, Penetration of intact
781 skin by quantum dots with diverse physicochemical properties, *Toxicol. Sci.* 91
782 (1) (2006) 159–165.
- 783 [48] O.E. Akilov, S. Kosaka, K. O'Riordan, T. Hasan, Parasitocidal effect of delta-
784 aminolevulinic acid-based photodynamic therapy for cutaneous leishmaniasis is
785 indirect and mediated through the killing of the host cells, *Exp. Dermatol.* 16 (8)
786 (2007) 651–660.
- 787 [49] C.D. Enk, C. Fritsch, F. Jonas, A. Nasereddin, A. Ingber, C.L. Jaffe, T. Ruzicka,
788 Treatment of cutaneous leishmaniasis with photodynamic therapy, *Arch.*
789 *Dermatol.* 139 (4) (2003) 432–434.
- 790 [50] K. Gardlo, S. Hanneken, T. Ruzicka, N.J. Neumann, Photodynamic therapy of
791 cutaneous leishmaniasis. A promising new therapeutic modality, *Hautarzt* 55 (4)
792 (2004) 381–383.
- 793 [51] K. Gardlo, Z. Horska, C.D. Enk, L. Rauch, M. Megahed, T. Ruzicka, C. Fritsch,
794 Treatment of cutaneous leishmaniasis by photodynamic therapy, *J. Am. Acad.*
795 *Dermatol.* 48 (6) (2003) 893–896.
- 796 [52] A. Asilian, M. Davami, Comparison between the efficacy of photodynamic therapy
797 and topical paromomycin in the treatment of Old World cutaneous leishmaniasis:
798 a placebo-controlled, randomized clinical trial, *Clin. Exp. Dermatol.* 31 (5) (2006)
799 634–637.
- 800 [53] O.E. Akilov, S. Kosaka, K. O'Riordan, T. Hasan, Photodynamic therapy for cutaneous
801 leishmaniasis: the effectiveness of topical phenothiaziniums in parasite eradica-
802 tion and Th1 immune response stimulation, *Photochem. Photobiol. Sci.* 6 (10)
803 (2007) 1067–1075.
- 804 [54] P. Escobar, I.P. Hernandez, C.M. Rueda, F. Martinez, E. Paez, Photodynamic activity
805 of aluminium (III) and zinc (II) phthalocyanines in *Leishmania promastigotes*,
806 *Biomedical* 26 (Suppl 1) (2006) 49–56.
- 807 [55] S. Dutta, D. Ray, B.K. Kolli, K.P. Chang, Photodynamic sensitization of *Leishmania*
808 *amazonensis* in both extracellular and intracellular stages with aluminum
809 phthalocyanine chloride for photolysis in vitro, *Antimicrob. Agents Chemother.*
810 49 (11) (2005) 4474–4484.
- 811 [56] J. Moan, K. Berg, The photodegradation of porphyrins in cells can be used to
812 estimate the lifetime of singlet oxygen, *Photochem. Photobiol.* 53 (4) (2001)
813 549–553.
- 814 [57] A.P. Castano, T. Demidova, M.R. Hamblin, Mechanisms in photodynamic therapy:
815 part one—photosensitizers, photochemistry and cellular localization, *Photodiagn.*
816 *Photodyn. Ther.* 1 (4) (2004) 279–293.
- 817 [58] C.A. Robertson, D.H. Evans, H. Abrahamse, Photodynamic therapy (PDT): a short
818 review on cellular mechanisms and cancer research applications for PDT, *J.*
819 *Photochem. Photobiol. B* 96 (1) (2009) 1–8.
- 820 [59] A. Ketabchi, A. MacRobert, P.M. Speight, J.H. Bennett, Induction of apoptotic cell
821 death by photodynamic therapy in human keratinocytes, *Arch. Oral Biol.* 43 (2)
822 (1998) 143–149.
- 823 [60] S. Coppola, L. Ghibelli, GSH extrusion and the mitochondrial pathway of apoptotic
824 signalling, *Biochem. Soc. Trans.* 28 (2) (2000) 56–61.
- 825 [61] R.M. Steinman, I.S. Mellman, W.A. Muller, Z.A. Cohn, Endocytosis and the recycling
826 of plasma membrane, *J. Cell Biol.* 96 (1) (1983) 1–27.
- 827 [62] A. Papagiannaros, C. Bories, C. Demetzos, P.M. Loiseau, Antileishmanial and
828 trypanocidal activities of new miltefosine liposomal formulations, *Biomed.*
829 *Pharmacother.* 59 (10) (2005) 545–550.
- 830 [63] P. Overath, Y.D. Stierhof, M. Wiese, Endocytosis and secretion in trypanosomatid
831 parasites – Tumultuous traffic in a pocket, *Trends Cell Biol.* 7 (1) (1997) 27–33.
- 832 [64] S.M. Landfear, M. Ignatushchenko, The flagellum and flagellar pocket of
833 trypanosomatids, *Mol. Biochem. Parasitol.* 115 (1) (2001) 1–17.
- 834 [65] G. Cevc, in: Lipowsky, Sachman (Eds.), *Handbook of Biological Physics*, Vol. I,
835 Elsevier Science BV, Amsterdam, 1995, pp. 465–489.
- 836 [66] P.L. Honeywell-Nguyen, J.A. Bouwstra, Vesicles as a tool for transdermal and
837 dermal delivery, *Drug Discov. Today: Technol.* 2 (1) (2005) 67–74.
- 838 [67] J.A. Cowen, R.E. Imhof, P. Xiao, Opto-thermal measurement of stratum corneum
839 renewal time, *Anal. Sci.* 17 (2001) s353–s356.
- 840 [68] J.P. Ryman-Rasmussen, J.E. Riviere, N.A. Monteiro-Riviere, Variables influencing
841 interactions of untargeted quantum dot nanoparticles with skin cells and
842 identification of biochemical modulators, *Nano Lett.* 7 (5) (2007) 1344–1348.